

Topological end states and Zak phase of rectangular armchair ribbon

Y. H. Jeong, S. -R. Eric Yang*

Department of Physics, Korea University, Seoul, Korea

Abstract

We consider the end states of a half-filled rectangular armchair graphene ribbon (RAGR) in a staggered potential. Taking electron-electron interactions into account we find that, as the strength of the staggered potential varies, three types of couplings between the end states can occur: antiferromagnetic without or with spin splitting, and paramagnetic without spin-splitting. We find that a spin-splitting is present only in the staggered potential region $0 < \Delta < \Delta_c$. The transition from the antiferromagnetic state at $\Delta = 0$ to the paramagnetic state goes through an intermediate spin-split antiferromagnetic state, and this spin-splitting disappears suddenly at Δ_c . For small and large values of Δ the end charge of a RAGR can be connected to the Zak phase of the periodic armchair graphene ribbon (PARG) with the same width, and it varies continuously as the strength of the potential changes.

Keywords: Graphene nanosystem, Fractional Charge, Edge magnetization, End state, Polarization, Zak phase.

1. Introduction

Graphene exhibits interesting fundamental physics[1], such as quantum Hall effect[2], Berry phases[3], and edge magnetism[4, 5]. End states, located at the end points of a long insulating one-dimensional wire[6], can reflect the presence of gap states with fractional properties and the nature of various electronic and magnetic bulk states. These objects are found in polyacetylene, spin chains, Kondo insulator, and other systems[7, 8, 9, 10, 11]. One may also ask whether an end charge exists in quasi-one-dimensional graphene ribbons and how it may be related to the Zak phase of the underlying band structure[12, 13].

A PAGR with the width $(3L + 1)a_0$ or $3La_0$ has an energy band gap and is semiconducting[16, 17, 14, 15, 18] (L is an integer and a_0 is the graphene unit cell length). On the other hand, an armchair ribbon with the width $(3L +$

*Corresponding author

Email address: eyang812@gmail.com (S. -R. Eric Yang)

2) a_0 and a zigzag ribbon do not have a gap in the absence of electron-electron interactions[17] (we will not consider these ribbons here). It is useful to think about a RAGR as generated from such a PAGR by cutting it transversely. A RAGR has two long armchair edges and two short zigzag edges[19, 20], see Fig.1. The left end of the RAGR is made of the A-type zigzag edge while the right end is made of the B-type. Gap states appear that are localized on the end sites[11], and their number grows with increasing length of the zigzag edges. In our work we will refer to these gap states as end states. Since the magnitude of the energy gap is sizable these states are isolated from other lower and higher energy quasi-continuum states. A staggered potential[21, 22, 23, 24] may modify the properties of end states of a RAGR, and the relation between the Zak phase of the PAGR and the end charge may also change.

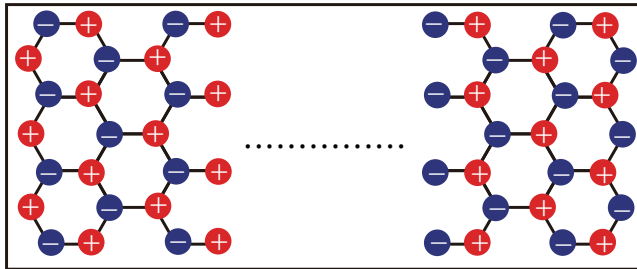


Figure 1: RAGR has two long armchair edges and two short zigzag edges. The lengths of the armchair and zigzag edges are, respectively, L_{arm} and L_{zig} (ribbon width W is equal to L_{zig}). The staggered potential energy is $\epsilon_i = \Delta/2$ on sublattice A (red circles) and $\epsilon_i = -\Delta/2$ on sublattice B (blue circles). Left (right) end is made of A (B)-type sites.

Our RAGR is assumed to be half-filled with an energy gap and its ribbon width is such that four spin-resolved gap states are present. Two of them are occupied while the other two are unoccupied. We find that the properties of the end states depend on the interplay between the strength of staggered potential, on-site repulsion, and ribbon length and width. As the strength of the staggered potential changes, we find three coupling types between the end states: antiferromagnetic without or with spin-splitting, and paramagnetic without spin-splitting. In this paper antiferromagnetic (ferromagnetic) gap states mean that their spins on opposite zigzag edges are coupled antiferromagnetically (ferromagnetically). Paramagnetic means zero net spin. The spin-splitting δ is defined as the energy difference between the highest occupied spin-up and -down gap states. Spin-splitting of the gap states is present only in the staggered potential region $0 < \Delta < \Delta_c$ (quasi-continuum states near the energy gap are also spin-split by a small amount). The transition from the antiferromagnetic state at $\Delta = 0$ to the paramagnetic state at Δ_c goes through an intermediate antiferromagnetic state whose gap states are spin-split. This spin-splitting vanishes abruptly at Δ_c . For $\Delta/t \gg 1$, where the hopping parameter is $t \sim 3eV$, and for some small Δ the value of the end charge can be connected to the Zak phase of

the PAGR with the same width, and the end charge varies continuously as the strength of the potential changes.

2. Band structure and Zak phase in a staggered potential

We would like to connect the end occupation numbers of a RAGR to the Zak phase of the band structure of the PAGR with the same ribbon length. We will investigate under what conditions they can be connected. We adopt a tight-binding model with on-site repulsion U and compute the band structure using the Hartree-Fock approximation(HFA)[25]. This approach is widely used and its results are consistent with those of DFT[4, 17, 26].

Figure 2 displays the HF band structure $E(k)$ in the presence of a staggered potential. The ground state is paramagnetic for various values of Δ and U used in this work, and no spin splitting of the occupied bands and no magnetization on the armchair edges are found. Bulk graphene band structure also does not show a band spin-splitting in a staggered potential[21]. But a periodic zigzag graphene ribbon does display a spin-splitting[24], and the presence of zigzag edges is important for the spin-splitting (note that our PAGR has no zigzag edges and end points). The size of the gap increases as the strength of the staggered potential increases. The computed band structure $E(k)$ is for the wave vector k is parallel to the ribbon axis. Note that the band structure has band crossings.

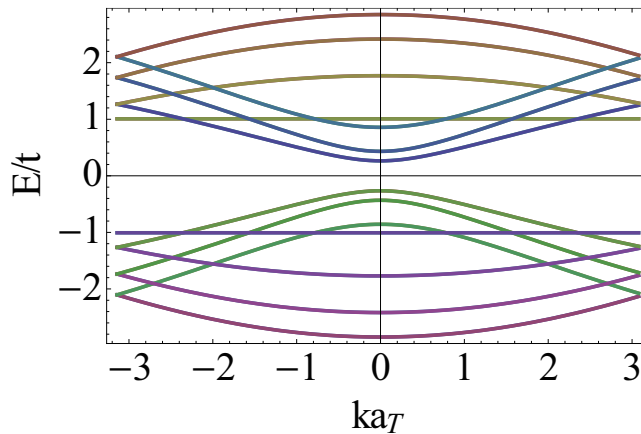


Figure 2: Band structure of a half-filled PAGR with width $W = 3a_0$ and the length of armchair edges $L_{arm} = 215.84 \text{ \AA}$ (Here a_0 is the unit cell length of the honeycomb lattice. The Fermi energy is $E_F = 0$). On-site potential is $U = 0.5t$ and staggered potential is $\Delta = 0.3t$. The length of the unit cell of the periodic ribbon is $a_T = 3a_{cc}$, where a_{cc} is the carbon-carbon distance.

” The band crossings and numerically computed eigenstates can give to states with wildly different phases, making it difficult to compute numerically the Zak

phase. Here we use a gauge invariant method[27]. Using the periodic part of the Bloch wavefunctions of the occupied bands we compute the spin-independent Zak phase

$$\mathcal{Z}/2\pi = \frac{1}{2\pi} \sum_{s=0}^{N_s-1} \text{Arg} [\det \langle C_{l,k_s} | C_{l',k_{s+1}} \rangle]. \quad (1)$$

The expansion coefficients $C_{l,k}$ are column vectors, whose components are the site indices $i = (m, A)$ or (m, B) , labeling atoms in the unit cell. They are obtained from our tight-binding Hamiltonian matrix,. Here, the Brillouin zone is divided into small intervals labeled by k_s . For each k_s , one computes all the matrix elements $\langle C_{l,k_s} | C_{l',k_{s+1}} \rangle$ (the matrix index l runs over the occupied bands).

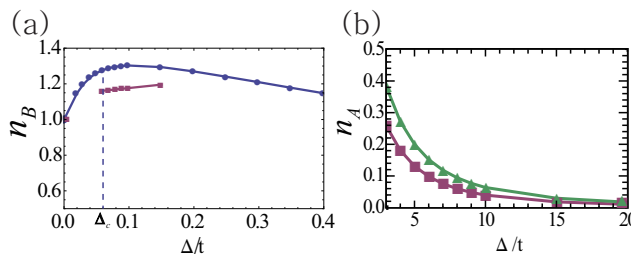


Figure 3: (a) Charge per right end site computed from the Zak phase (circles) and from the occupation number (squares) in the region $\Delta/t < 1$. (b) Charge per left end site computed from the Zak phase (triangles) and from the occupation number (squares) in the region $\Delta/t \gg 1$. Parameters are identical to those of Fig.2.

For an *insulating interface* of a RAGR the total end charge per spin is related to the Zak phase of the PAGR: $Q/e = \frac{\mathcal{Z}}{2\pi}$ [13]. Note that due to gauge invariance the phase Z is only defined within mod 2π . The occupation number per site $n_{A,B}$ is obtained by dividing Q/e with the total number N of A or B end sites. The condition for an insulating interface is that the average end occupation number per A-site is $n_A \approx 0$ or $n_A \lesssim 1$, corresponding, respectively, to $\Delta/t \gg 1$ or $\Delta \rightarrow 0$ (the condition for the B-sites is $n_B \gtrsim 1$ or $n_B \approx 0$). Figure 3 shows results of n_B computed from the Zak phase and from the numerical calculation of the occupied wavefunctions. As shown in Fig.3 (a), at $\Delta = 0$ they agree with each other: $n_B = 1$ (the Zak phase of each spin is 0 mod 2π). In the region $\Delta/t \gg 1$ the two agree as Δ/t increases, see Fig.3 (b). However, for $0 < \Delta < \Delta_c$ our numerical result indicates that the comparison between the two approaches cannot be made ($\Delta_c = 0.06t$). This is because, the gap states and the quasi-continuum states of the RAGR near the gap are spin-split while all the states of the PAGR are spin degenerate (spin-splitting and occupation numbers are computed below). In the region $\Delta \gtrsim \Delta_c$ the agreement between

the two approaches for the B-end site is within 15 – 20%, as shown in Fig.3 (a). Note that the value of the occupation number is somewhat larger than one: the spin down ($\sigma = -1$) part contributes 1 to n_B and the opposite spin ($\sigma = 1$) part accounts for the remaining part.

3. Antiferromagnetic and paramagnetic couplings

In RAGRs the antiferromagnetic, paramagnetic, antiferromagnetic with broken sublattice symmetry, and ferromagnetic states compete against each other. To compute the end charges, magnetization, and spin-splitting of our RAGR we use the following approach. Since translational symmetry is broken we write a tight-binding Hamiltonian in the site representation including the on-site repulsion U . We solve it using the Hartree-Fock (HF) approximation (the dimension of the Hamiltonian matrix is ~ 1400). In general the nature of the ground state depends on the interplay between several parameters Δ , U , t , L_{zig} , and L_{arm} . We investigate RAGRs with a short width, $\frac{L_{zig}}{L_{arm}} \ll 1$. The end electrons interact with the bulk electrons and a many-body calculation is required. We compute the average end occupation number per A-site of the left zigzag edge: $n_A = \sum_{\sigma} n_{A,\sigma} = \frac{1}{N} \sum_{\sigma} \sum_{\alpha \in occ, i} |\psi_{A,\sigma}^{\alpha}|^2$, where the sum is over the occupied states α , spin states σ , and site index i ($\psi_{i,A}^{\alpha}$ are the probability amplitudes). Note that, in addition to occupied gap states, there are also occupied quasi-continuum states that have to be included in the sum. At a B-site on the opposite end the occupation number n_B is defined similarly. The average per site magnetizations on the left and right zigzag edges are, respectively, $m_A = n_{A,\uparrow} - n_{A,\downarrow}$ and $m_B = n_{B,\uparrow} - n_{B,\downarrow}$.

In Fig.4 we have computed, as a function of Δ , the spin-splitting of the gap states of the ground state. It indicates that a sudden electronic and magnetic reconstruction of the end states occurs near Δ_c . At $\Delta = 0$ we find that the ground state is antiferromagnetic without spin-splitting (however, there is a ferromagnetic state whose energy nearly degenerate[19]). In the interval $0 < \Delta < \Delta_c$ the ground state is antiferromagnetic but with spin-splitting. For $\Delta > \Delta_c$ the ground state is paramagnetic without spin-splitting.

To explain the abrupt change we need to investigate what types of gap states are occupied as Δ changes. Figure 5 displays the computed energy spectra for spin-up and -down gap states and quasi-continuum states outside the gap. Figure 6 displays the schematic probability densities of the occupied gap states. For $\Delta < \Delta_c$ the spin-up and -down gap states are located, respectively, on the left and right end sites (see Figs.5(a) and 6(a)). In this case the occupied spins of the gap states are coupled antiferromagnetically. Note that near the critical value Δ_c the spin-up gap states are nearly degenerate, see Fig.5(a). On the other hand, for $\Delta > \Delta_c$ both are localized on the right end sites, as shown in Figs.5(b) and 6(b). The antiferromagnetism vanishes. At the critical value Δ_c an electron localized on the left edge, transfers to the right end sites, where the potential energy is lower. However, there is also an accompanying rearrangement of the occupied quasi-continuum states, and the resulting total charge transfer to the right end sites may not be entirely one. For $\Delta \gtrsim \Delta_c$ the occupation per site

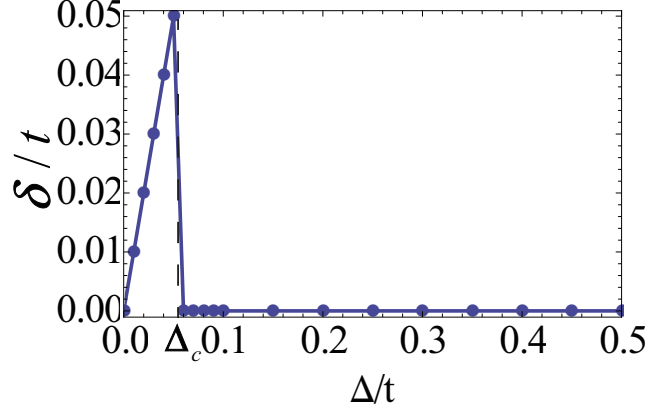


Figure 4: Spin-splitting of gap states δ of a RGAR is shown (δ is defined in Sec.1). On-site potential is $U = 0.5t$, width $L_{zig} = 3a_0$, and ribbon length $L_{arm} = 215.84 \text{ \AA}$.

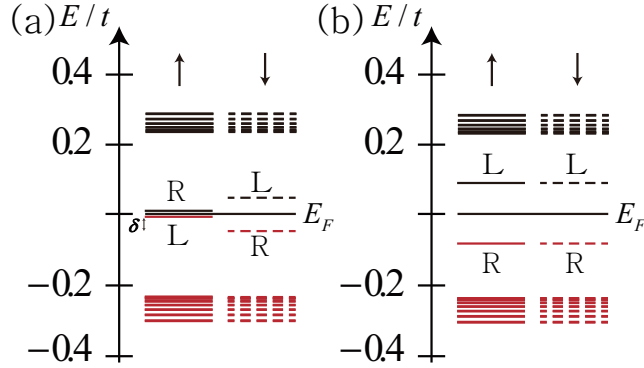


Figure 5: Schematic drawing of energy spectrum for spin-up and -down end/gap states of a RAGR with width $L_{zig} = 3a_0$. Two values of the strength of the staggered potential, $0.03t$ (a) and $0.3t$ (b), are used. The first value is just below the critical value Δ_c and the second one is far above it. Spin splitting δ is present in (a) while not in (b). In (a) the occupied end states are located on the opposite zigzag edges (see Fig.6(a)). While in (b) they are both located on the right zigzag edge (see Fig.6(b)). Symbols R and L mean that an end state is localized, respectively, on the right and left zigzag edges.

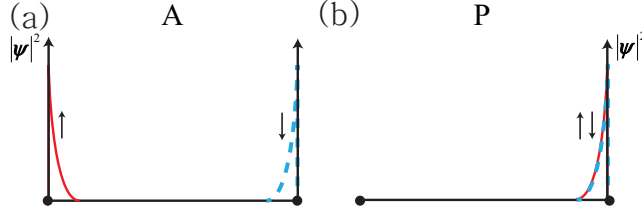


Figure 6: Schematic probability densities of the occupied end states are displayed. They are located either on the left or right end sites. Staggered potential energy is lower on the right end sites. (a) End states are located on opposite end sites with antiparallel spins: antiferromagnetism; (b) end states are located on the same end sites with antiparallel spins: paramagnetism.

is somewhat less than $n_B = 4/3$, but it quickly approaches this value as Δ increases and the total electron number on the three B-end sites becomes 4, consistent with one extra electron on the right edge. The magnetization m_A is almost not changing until Δ_c , where it suddenly decreases to zero from a positive value. Also the magnetization m_B is not changing until Δ_c , where it increases abruptly to zero from a negative value. Below $\Delta < \Delta_c$ the sum is $m_A + m_B = 0$, consistent with antiferromagnetism.

4. Summary and discussions

We have shown that for the values of the staggered potential $\Delta/t \gg 1$ and for some small Δ the end charge of a RAGR can be connected to the Zak phase of the PAGR with the same width. The computed end charge varies continuously on the strength of the potential. The comparison between the two quantities cannot be made in the region $0 < \Delta < \Delta_c$ because the gap states and the quasi-continuum states near the gap of the RAGR display spin-splitting while those of the PAGR do not.

As the strength of the staggered potential varies we find that the end states of a RAGR can be divided into three magnetic coupling regimes: antiferromagnetic without or with spin-splitting, and paramagnetic without spin-splitting. The transition from the antiferromagnetic state at $\Delta = 0$ to the paramagnetic state goes through an intermediate antiferromagnetic state with spin-splitting. The spin-splitting disappears suddenly at Δ_c .

We have performed the HF calculations with larger widths and lengths of the rectangular ribbon than those used in Fig.3. We find that, although a longer zigzag edge produces more gap states, the dependence of the end charge on the strength of the staggered potential is qualitatively similar to the result for shorter zigzag edges: at $\Delta = 0$ the occupation number per site is one and at a critical value Δ_c paramagnetism appears. In the absence of the staggered potential ($\Delta = 0$) inversion symmetry is intact and the Zak phase is $0 \bmod 2\pi$, independent of the range of electron-electron interactions. At $\Delta \neq 0$, where inversion symmetry of the electronic density of the ground state is broken, there

may be some quantitative differences between the results of the short-range and long-range interactions. But, as we mentioned before, the results of a short-range model are expected to be in qualitative agreement with those of a first principles calculation of graphene nanoribbons using the long-range Coulomb interactions, see refs. [17, 26]. Moreover, the HF treatment of the long-range Coulomb interactions in bulk two-dimensional graphene leads to the renormalization of the band structure with only slight deviations from the linear behavior with unchanged electronic wavefunctions[25].

It may be worthwhile to find ways to modulate the end/gap states by strain or electric field. The measurement of the differential conductance, using scanning tunneling microscopy[28], may provide rich information on the end states.

Acknowledgments

This research was supported by Basic Science Research Program through the National Research Foundation of Korea(NRF) funded by the Ministry of Education, ICT & Future Planning(MSIP) (NRF-2015R1D1A1A01056809).

References

- [1] A. H. Castro Neto, F. Guinea, N. M. R. Peres, K. S. Novoselov, and A. K. Geim, *Rev. Mod. Phys.* **81**, 109 (2009).
- [2] Y. Zhang, Y.-W. Tan, H. L. Stormer, and P. Kim, *Nature* **438**, 201 (2005).
- [3] T. Ando, *J. Phys. Soc. Jpn.* **74**, 777 (2005).
- [4] M. Fujita, K. Wakabayashi, K. Nakada, K. Kusakabe, *J. Phys. Soc. Jpn.*, **65**, 1920 (1996).
- [5] Y. W. Son, M. L. Cohen, and S. G. Louie, *Nature* **444**, 347 (2006).
- [6] A. Y. Kitaev, *Usp. Fiz. Nauk* **171**, 131 (2001).
- [7] A. J. Heeger, S. Kivelson, J. R. Schrieffer, and W.-P. Su, *Rev. Mod. Phys.* **60**, 781 (1988).
- [8] H.M. Guo and S. Q. Shen, *Phys. Rev. B* **84**, 195107 (2011).
- [9] T.K. Ng, *Phys. Rev. B* **50**, 555 (1994).
- [10] V. Alexandrov and P. Coleman, *Phys. Rev. B* **90**, 115147 (2014).
- [11] Y. H. Jeong, S.C. Kim, and S.-R. Eric Yang, *Phys. Rev. B* **91**, 205441 (2015).
- [12] J. Zak, *Phys. Rev. Lett.* **62**, 2747 (1989).
- [13] D. Vanderbilt and R. D. King-Smith, *Phys. Rev. B* **48**, 4442 (1993).

- [14] B. Trauzettel, D. V. Bulaev, D. Loss and G. Burkard, *Nature Physics* **3**, 192 (2007).
- [15] J. Cai, P. Ruffieux, R. Jaafar, M. Bieri, T. Braun, S. Blankenburg, M. Muoth, A. P. Seitsonen, M. Saleh, X. Feng, K. Müllen, and R. Fasel, *Nature* **466**, 470 (2010); T. Kato and R. Hatakeyama, *Nat. Nanotech.* **7**, 651 (2012).
- [16] L. Brey and H. A. Fertig, *Phys. Rev. B* **73**, 235411 (2006).
- [17] L. Yang, C.-H. Park, Y.-W. Son, M. L. Cohen, and S. G. Louie, *Phys. Rev. Lett.* **99**, 186801 (2007).
- [18] J. W. Lee, S. C. Kim, and S. -R. Eric Yang, *Solid State Commun.* **152**, 1929 (2012).
- [19] C. Tang, W. Yan, Y. Zheng, G. Li, and L. Li, *Nanotechnology* **19**, 435401 (2008).
- [20] S.C. Kim, P.S. Park, and S.-R. Eric Yang, *Phys. Rev. B* **81**, 085432 (2010)
- [21] S. Y. Zhou, G.-H. Gweon, A. V. Fedorov, P. N. First, W. A. de Heer, D.-H. Lee, F. Guinea, A. H. Castro Neto, and A. Lanzara, *Nature Materials* **6**, 770 (2007).
- [22] C.R. Dean, A.F. Young, I. Meric, C. Lee, L. Wang, S. Sorgenfrei, K. Watanabe, T. Taniguchi, P. Kim, K.L. Shepard, and J. Hone, *Nature Nanotechnology* **5**, 722 (2010).
- [23] J. Xue, J. Sanchez-Yamagishi, D. Bulmash, P. Jacquod, A. Deshpande, K. Watanabe, T. Taniguchi, P. Jarillo-Herrero, and B. J. LeRoy, *Nature Materials* **10**, 282 (2011).
- [24] D. Soriano and J. Fernández-Rossier, *Phys. Rev. B* **85**, 195433 (2012).
- [25] T. Stauber, P. Parida, M. Trushin, M. V. Ulybyshev, D. L. Boyda, and J. Schliemann *Phys. Rev. Lett.* **118**, 266801(2017).
- [26] L. Pisani, J. A. Chan, B. Montanari, and N. M. Harrison, *Phys. Rev. B* **75**, 064418 (2007).
- [27] R. Resta, *Rev Mod Phys.* **66**, 899 (1994).
- [28] E. Y. Andrei, G. Li, and X. Du, *Rep. Prog. Phys.* **75**, 056501 (2012).